HHS Public Access

Author manuscript

Obesity (Silver Spring). Author manuscript; available in PMC 2025 January 01.

Published in final edited form as:

Obesity (Silver Spring). 2024 January ; 32(1): 120–130. doi:10.1002/oby.23929.

Adipocyte retinoic acid receptor alpha prevents obesity and steatohepatitis by regulating energy expenditure and lipogenesis

Fathima N. Cassim Bawa[1,*], **Shuwei Hu**[1,*], **Raja Gopoju**[1], **Amy Shiyab**[1], **Kai Mongan**[1], **Yanyong Xu**[1,#], **Xiaoli Pan**[1], **Alyssa Clark**[1], **Hui Wang**[1], **Yanqiao Zhang**[1]

[1]Department of Integrative Medical Sciences, Northeast Ohio Medical University, Rootstown, OH, 44272, USA

Abstract

Objective: The adipose tissue-liver axis is a major regulator of the pathogenesis of non-alcoholic fatty liver disease (NAFLD). Retinoic acid signaling plays an important role in development and metabolism. However, little is known about the role of adipose retinoic acid signaling in the development of obesity-associated NAFLD. In this work, we aimed to investigate whether and how retinoic acid receptor alpha (RARα) regulated the development of obesity and NAFLD.

Methods: RARα expression in adipose tissue of *db/db* or *ob/ob* mice was determined. $Rara^{fl/fl}$ mice and adipocyte-specific $Rara^{-/-}$ ($Rara^{Adi-/-}$) mice were fed a chow diet for one year or high fat diet (HFD) for 20 weeks. Primary adipocytes and primary hepatocytes were co-cultured. Metabolic regulation and inflammatory response were characterized.

Results: RARα expression was reduced in adipose tissue of *db/db* or *ob/ob* mice. $Rara^{Adi-/-}$ mice had increased obesity and steatohepatitis (NASH) when fed a chow diet or HFD. Loss of adipocyte *Rara* induced lipogenesis and inflammation in adipose tissue and the liver and reduced thermogenesis. In the co-culture studies, loss of *Rara* in adipocytes induced inflammatory and lipogenic programs in hepatocytes.

Conclusions: Our data demonstrate that RARα in adipocytes prevents obesity and NASH via inhibiting lipogenesis and inflammation and inducing energy expenditure.

Keywords

Steatohepatitis; RARalpha; adipose tissue; lipogenesis; energy expenditure

Corresponding author: Dr. Yanqiao Zhang, Department of Integrative Medical Sciences, Northeast Ohio Medical University, 4209 State Route 44, Rootstown, Ohio 44272, USA. Phone 330.325.6693. yzhang@neomed.edu.

[#]Current address: Key Laboratory of Metabolism and Molecular Medicine of the Ministry of Education, Department of Pathology of School of Basic Medical Sciences, Fudan University, Shanghai, China

[*]These authors contributed equally to this work.

Author contributions

F.N.C.B and Y. Zhang conceived and designed the studies and interpreted the results. Y. Zhang supervised the project. F.N.C.B and Y. Zhang prepared the manuscript. S.H. performed several *in-vivo* and *in-vitro* studies. R.G., K.M., A.S., X.P., A.K., H.W. and Y.X. performed various studies. All authors discussed the results and approved the final version of the manuscript.

Conflicts of interest: The authors declare no conflicts of interest exist.

Introduction

There has been a significant increase in the obesity rate in the last 50 years. It is currently the second leading cause of preventable death in the United States and represents a significant global health concern (1, 2). Obesity has been associated with many health risks, including a spectrum of liver abnormalities known as nonalcoholic fatty liver disease (NAFLD), which encompasses nonalcoholic fatty liver (NAFL) and non-alcoholic steatohepatitis (NASH). Adipose tissue secretes various hormones such as adipokines, cytokines, and metabolites. Under over-nutritional conditions, pathological remodeling of adipose tissue results in increased secretion of toxic fatty acids and inflammatory cytokines while reducing the secretion of anti-inflammatory adipokines, such as adiponectin, which may in turn have deleterious effects on the pathogenesis of obesity-associated NAFLD.

Vitamin A deficiency is often associated with insulin resistance and obesity. An inverse correlation is observed between obesity and vitamin A status in people with obesity (3, 4). Multiple studies on patients have shown an inverse relationship between serum retinol levels and the severity of NAFLD (5–7). Vitamin A exerts its functions through active metabolites – all-trans retinoic acid (AtRA) and 9-cis retinoic acid (9-cis-RA) which activate the nuclear hormone receptors retinoic acid receptors (RARα, RARβ, and RARγ) and retinoid X receptors (RXRα, RXRβ, and RXRγ), respectively (8, 9). RARs heterodimerize with RXR and bind to the DNA motifs known as retinoic acid response elements (RAREs) to regulate the expression of genes involved in cell growth, differentiation, and metabolism (10). Lee *et al.* have previously observed that adipocyte-specific over-expression of dominant-negative RARα increases insulin intolerance and hepatic steatosis in chow-fed mice supplemented with Vitamin A (11). However, the underlying mechanism remains to be determined. In addition, it is unclear whether genetic ablation of adipocyte RARα and/or a high fat diet (HFD) have similar effects or an effect on NASH development.

In this report, we show that adipose RARα was reduced in genetically obese mice. We then investigated the effect of genetic ablation of adipocyte RARα on the development of obesity and NAFLD in mice fed a chow diet or HFD. Our data show that adipocyte RARα is essential for protecting against obesity and NASH by regulating energy expenditure and lipogenesis.

Methods

Mice and diets

C57BL/6J mice (cat # 000664), *ob/ob* mice (cat # 000632) and *db/db* mice (cat # 000697) were purchased from the Jackson Laboratories (JAX; Bar Harbor, ME). The floxed *Rara* (*Rara*$^{fl/fl}$) mice on a C57BL/6 background were generously gifted by Dr. Yasmine Balkaid (NIH/NIAID) and have been described previously by Dr. Chambon and colleagues (12). *Rara*$^{fl/fl}$ mice were crossed with Adiponectin (Adipoq) cre mice (strain # 010803) from JAX to generate germline adipocyte-specific *Rara*$^{-/-}$ (*Rara*$^{Adi-/-}$) mice and control littermates (*Rara*$^{fl/fl}$ mice). All mice were housed in ventilated microisolator cages with Aspen shred bedding and nestlets and paper huts, and in a temperature and humidity-controlled room with a 12-h light/12-h dark cycle under pathogen-free conditions. Mice were randomly

assigned for studies, and were fasted for 5–6 hours during the light cycle prior to euthanasia. Plasma and tissues such as liver, epididymal white adipose tissue (eWAT), inguinal white adipose tissue (iWAT), and brown adipose tissue (BAT) were collected. All the animal experiments were approved by the Institutional Animal Care and Use Committee at Northeast Ohio Medical University (NEOMED), and all the procedures were in accordance with the ARRIVE guidelines. No animals were excluded. Eight-week-old male mice were used and fed with a high fat diet (HFD) containing 60% fat (cat # D12492 from Research Diets, New Brunswick, NJ) for 20 weeks or a chow diet for one year.

Cell culture

3T3L1 cells were purchased from ATCC and were grown in Dulbecco's Modified Eagle Medium (DMEM) supplemented with 10% fetal bovine serum and 1% antibiotic and antimycotic. Adipogenesis was induced as detailed in the Supplementary Information.

Body composition analysis and energy expenditure

Mouse body fat mass was measured by Echo-MRI-700 (Echo Medical Systems, Houston, TX). Oxygen consumption, carbon dioxide production, heat production, and physical activity were determined in a Comprehensive Lab Animal Monitoring System (CLAMS) using Columbus Instruments hardware and Oxymax software (Columbus Instruments, Columbus, OH), as detailed previously (13). In brief, mice underwent an acclimation period, and over 50 hours measurement of energy expenditure was determined using an eight-chamber system. Each run included two genotypes with four mice per group.

Quantitative real-time PCR

RNA was extracted using TRIzol reagent and real-time PCR was performed as detailed in Supplementary Information.

Western blot assays

Western blot assays were performed using lysates from tissues or primary adipocytes. Samples were homogenized in a solution containing 50 mM Hepes (pH 7.5), 137 mM NaCl, 1 mM $MgCl_2$, 1 mM $CaCl_2$, 10 mM sodium pyrophosphate, 10 mM sodium fluoride, 2 mM EDTA, 1% Nonidet P-40, 1 mM PMSF and complete protease and phosphatase inhibitor mixture (Fisher Scientific) and then incubated at 4°C for 30 minutes. After centrifugation at 15,000 × *g* for 30 min, the supernatant was removed, and protein concentration was determined. Proteins were separated on SDS/PAGE and transferred to a nitrocellulose membrane. Antibodies against acetyl-CoA carboxylase (ACC) (cat # 3662), phospho-AMP-activated protein kinase (pAMPK) (cat # 2535), AMP-activated protein kinase (AMPK) (cat # 2603), phospho-hormone sensitive lipase (pHSL) (cat # 45804), hormone-sensitive lipase (HSL) (cat # 4107), adipose tissue triglyceride lipase (ATGL) (cat # 2138), uncoupling protein 1 (UCP1) (cat # 14670), phospho serine/threonine kinase 1 (pAKT) (cat # 4060), total AKT (cat # 9272), cleaved caspase 3 (Cat # 9661), total caspase 3 (Cat # 9662), phospho-Smad2/3 (Cat # 8828), or total Smad2/3 (Cat # 5678) were purchased from Cell Signaling Technology (Boston, MA). The antibody against sterol regulatory element-binding protein 1 (SREBP-1) (cat # NB600–582) was purchased from Novus (Centennial, CO).

Retinoic acid receptor alpha (RARα) (cat # sc-515796) antibody was purchased from Santa Cruz Biotechnology (Dallas, TX). The antibody against tubulin (cat # ab4074) was purchased from Abcam (Waltham, MA). The anti-tubulin antibody was used at a 1:5000 dilution, and other primary antibodies were used at a 1:1000 dilution. Western blot images were collected by the Amersham Imager 680. Quantification of immunoblots was performed using ImageJ.

Analysis of AST, ALT, and lipid levels

Plasma AST and ALT levels were determined using Infinity reagents from Thermo Scientific. For the hepatic lipids, about 100 mg of liver was homogenized in methanol, and lipids were extracted in chloroform/methanol (2:1 v/v) as described previously (14). Hepatic triglyceride levels were quantified using Infinity reagents from Thermo Scientific (Waltham, MA). Plasma and hepatic non-esterified free fatty acids (NEFA) were determined using a kit from Wako Chemicals USA (Richmond, VA).

Analysis of hepatic hydroxyproline, reactive oxygen species, and DNA fragmentation

Hepatic hydroxyproline level was quantified using a kit from Cell BioLabs (cat # STA675). Hepatic reactive oxygen species (ROS) were measured using the OxiSelect In Vitro ROS/RNS Assay kit (cat # STA-347) from Cell Biolabs according to manufacturer's instructions. Liver DNA fragmentation (e.g., apoptosis) was determined using a terminal deoxynucleotidyl transferase dUTP nick end labeling (TUNEL) kit (cat # ab206386) from Abcam according to manufacturer's instructions.

Oil Red O (ORO), hematoxylin and eosin (H&E) or Picrosirius red staining

Liver and adipose tissues were fixed in 10% formalin, embedded in paraffin, and stained with H&E. The adipocyte size was calculated using ImageJ. Liver sections were also stained with Picrosirius red. For Oil Red O staining, liver tissues were fixed in 10% formalin and embedded in OCT and stained with Oil Red O. Images were acquired using an Olympus microscope.

F4/80 Immunohistochemical staining

Immunohistochemical staining of F4/80 in the formalin-fixed liver and WAT tissues was used for immunohistochemical staining of F4/80 (Abcam, cat # ab6640) was performed using Immunocruz ABC Staining Kit (cat # sc-2018) and DAB Peroxidase Substrate Kit (Vector Laboratories, Inc., Burlingame, CA) according to the manufacturer's instructions. The F4/80 antibody was purchased from Abcam (cat # ab6640). F4/80-positive area (%) was quantified using Image Pro (Media Cybernetics)

Ex vivo lipolysis assay

Lipolysis in white adipose tissue (WAT) was measured using the method described previously (15). About 50–60 mg inguinal fat pads were incubated for 2 hours at 37 °C in 2% fatty acid-free BSA with or without 10 μm isoproterenol. After inactivation at 65 °C for 10 min, glycerol release was determined using a kit from Sigma (cat # MAK117–1KT) and non-esterified free fatty acids (NEFAs) were determined using reagents from Wako

Chemicals (cat # 995–34791/991–34891). The basal lipolysis at 0 h and induced lipolysis rates at 2 h were normalized to proteins.

Glucose or insulin tolerance tests

Glucose tolerance test (GTT) was performed after mice were fasted overnight followed by intraperitoneal injection of 2 g/kg glucose. Insulin tolerance test (ITT) was performed after mice were fasted for 6 h followed by intraperitoneal injection of 0.8 U/kg insulin. Blood glucose levels were measured using a glucometer at the indicated time points.

Isolation of stromal vascular fraction (SVF) and differentiation into adipocytes

Primary pre-adipocytes were isolated from WAT and BAT of $Rar\alpha^{fl/fl}$ and $Rar\alpha^{Adi-/-}$ mice as previously described with some modifications and differentiated into mature adipocytes (16). Detailed information on SVF isolation and adipocyte differentiation is provided in the Supplementary Information.

Primary peritoneal macrophage isolation

Primary peritoneal macrophages were isolated as described previously (17). Briefly, mice were injected i.p. with sterile 4% Brewer's thioglycolate medium. After 4 days, peritoneal macrophages were isolated from the peritoneal cavity using cold phosphate-buffered saline (PBS). Macrophages were separated after centrifugation and resuspended in cell culture medium.

De novo lipogenesis in adipocytes

Primary pre-adipocytes that underwent induction of adipogenesis were incubated in serum-free DMEM in a 6-well plate for 2 hours, and then incubated for 2 hours in the presence of 0.5 μCi ^{14}C-acetate (PerkinElmer) plus 10 μM cold acetate. After washing twice with PBS, cells were collected in 0.1 N HCl. Lipids were extracted in 500 μl of 2:1 chloroform/methanol (v/v). The radioactivity in the lipid layer was determined by scintillation counting and normalized to protein levels.

Microplate-based respirometry

Cellular oxygen consumption was measured at 37 °C with an XFe24 Extracellular Flux Analyzer as previously published (18). Primary preadipocytes were isolated and plated on an XFe24 cell culture microplate. Detailed information on respirometry and UCP-dependent respiration is presented in Supplementary Information.

Primary hepatocyte isolation and co-culture

Mouse primary hepatocytes were isolated and co-cultured with mature adipocytes as described (19). Mice were anaesthetized by intraperitoneal injection of xylazine/ketamine. The portal vein was cannulated with a 23-gauge plastic cannula. Mouse livers were perfused with Hank's Balanced Salt Solution (HBSS, 14170112, Thermo Fisher Scientific). Subsequently, livers were perfused with HBSS with calcium and magnesium (14025092, Thermo Fisher Scientific) containing 0.8 mg/mL collagenase (Clostridium histolyticum type IV, Sigma, St. Louis, MO). Primary hepatocytes were released and collected in a 50-mL

centrifuge tube. After centrifugation at 50 × *g* for 3 minutes and washing with DMEM, cells were cultured in DMEM plus 10% FBS in collagen-coated PTFE- membrane inserts of 0.4 μM pore size (Cat # 3493, Corning). The inserts were placed in 6-well plates containing mature adipocytes (3T3L1 cells with induced adipogenesis). 6 hours after plating primary hepatocytes the medium was replaced with new medium. After 48 hours of plating, the primary hepatocytes were collected for downstream experiments.

Enzyme-linked immunosorbent assay (ELISA)

Plasma levels of TNFα (Cat # 900-M54) and MCP1 (Cat # 900-M126) were measured using ELISA kits from Peprotech. Plasma adiponectin (cat # MRP300) and IL-1β (Cat# DY401) levels were measured using ELISA kits from R&D Biosystems.

Promoter-luciferase assays

The pGL3-Ucp1-2.3kb plasmid was obtained from Dr. Laurent VERGNES (20) (University of California Los Angeles, Los Angeles, CA) and the pGL3-Adipq-3kb plasmid was provided by Dr. Jianhua Shao (University of California San Diego, La Jolla, CA). 3T3L1 cells were transfected with the pGL3 luciferase plasmid and CMV-β-galactosidase plasmid together with CMV-Null or CMV-RARα plasmids, and treated with either vehicle or 2 μM of AM580 (an RARα specific agonist) overnight. Luciferase activity was assayed using Bright-Glo luciferase assay system (Promega) and normalized to β-galactosidase activity.

Hepatic fatty acid composition

Briefly about 160 mg liver was homogenized in methanol and lipids were extracted in chloroform/methanol (2:1 v/v) as described previously (14). Detailed information on hepatic fatty acid composition is presented in Supplementary Information.

Hepatic de novo palmitate and triglyceride (TG) synthesis

$Rara^{fl/fl}$ and $Rara^{Adi-/-}$ mice were given an HFD for 12 weeks. During the last week, the mice were given 8% $^{2}H_{2}O$ in the drinking water. Detail information on hepatic de novo palmitate and TG synthesis is presented in the Supplementary Information.

Statistical analysis

Sample size was calculated based on our previous studies and power analysis. All data were expressed as mean ± SEM. Statistical significance was analyzed using unpaired student t-test or analysis of variance (ANOVA; for more than two groups) (GraphPad Prism, CA). Analysis of covariances (ANCOVA) for the indirect calorimetry study was carried out using CalR through the website (https://CalRapp.org/) as described (21). Differences were considered statistically significant at $P<0.05$.

Results

Adipocyte RARα deficiency exacerbates HFD-induced obesity

A previous report showed that *RARα* mRNA was reduced by 56% in subcutaneous adipose tissue of obese people (22). In genetically obese *ob/ob* mice, RARα protein levels in WAT

or BAT were reduced by >70% (Figure 1A–B). Similar results were observed in genetically obese *db/db* mice (Figure 1C–D). Our data also show that in addition to adipocytes, RARα was also expressed in the stromal vascular fraction (SVF) and macrophages to higher or comparable levels (Figure 1E).

To address the role of adipose RARα in metabolism, we generated $Rar\alpha^{Adi-/-}$ mice and the control littermates ($Rar\alpha^{fl/fl}$ mice) by crossing $Rar\alpha^{fl/fl}$ mice with Adipoq-Cre mice, which were then fed an HFD for 20 weeks. $Rar\alpha^{Adi-/-}$ mice had increased body weight and obesity (Figure 2A), increased body fat content and eWAT and iWAT weight (Figure 2B), enlarged adipocyte size in eWAT and iWAT (Figure 2C–D), and increased perilipin 1 (*Plin1*) expression in WAT (Figure 2E). In pre-adipocytes isolated from $Rar\alpha^{Adi-/-}$ mice, *Plin1* and *Plin3* mRNA levels were also significantly increased (Figure 2F). Thus, the gene expression data support the finding of the enlarged adipocytes in $Rar\alpha^{Adi-/-}$ mice.

Adipocyte RARα deficiency reduces energy expenditure and UCP-dependent thermogenesis

Impaired energy metabolism is known to contribute to obesity. To define the role of adipocyte RARα in energy metabolism, at the 16th week of HFD we performed indirect calorimetry experiments using CLAMS. The loss of adipocyte RARα led to decreased energy expenditure (Figure 3A, left and right panels) and expression of genes involved in thermogenesis, including uncoupled protein 1 (*Ucp1*), *Ucp2*, *Ucp3*, PR domain containing 16 (*Prdm16*), and peroxisome proliferator-activated receptor γ coactivator 1α (*Pgc1α*) (Figure 3B). Western blot assays showed that $Rar\alpha^{Adi-/-}$ mice had a >50% reduction in UCP1 and phospho-AKT (pAKT) protein levels in BAT (Figure 3C). There was no change in respiratory exchange ratio (RER), activity or food intake (Figure S1A–B). In addition, loss of adipocyte RARα increased glucose intolerance but had little impact on insulin tolerance (Figure 3D).

We next determined oxygen consumption rate (OCR) using a Seahorse XFe24 Flux Analyzer in primary brown adipocytes via the sequential injection of oligomycin, isoproterenol, FCCP, and antimycin (Figure 3E, left panel). We included isoproterenol in the injections as it stimulates lipolysis to release free fatty acids (FFAs), which in turn increase UCP1-mediated leak respiration (23). Loss of RARα reduced UCP-dependent OCR by 86% (Figure 3E, right panel), highlighting an important role of RARα in regulating UCP1 expression. In 3T3L1 cells, treatment with AM580, a specific RARα agonist, significantly increased *Ucp1* promoter-luciferase activity (Fig 3F). Together, the data of Figure 3 suggest that loss of adipocyte RARα increases obesity likely through impairing UCP-mediated thermogenesis.

Adipocyte RARα deficiency exacerbates HFD-induced hepatic lipid accumulation through inducing lipogenesis

Obesity-associated NAFLD is one of the most common liver diseases. On an HFD, $Rar\alpha^{Adi-/-}$ mice had elevated levels of hepatic triglycerides (TG) and non-esterified fatty acids (NEFA) (Figure 4A, left and middle panels). Analysis of fatty acid composition by GC-MS showed that $Rar\alpha^{Adi-/-}$ mice had increased C14:0, C16:0, C16:1, C18, C18:1,

C18:2, C18:3, C20:0, and C20:4 fatty acid levels (Figure 4A, right panel). Histological staining showed that *Rarα*$^{Adi-/-}$ mice had increased lipid accumulation in the liver (Figure 4B). qRT-PCR studies showed that hepatic genes involved in lipogenesis or fatty acid uptake were induced, including sterol regulatory element-binding protein 1c (*Srebp1c*), fatty acid synthase (*Fasn*), acetyl-CoA carboxylase 2 (*Acc2*), and fatty acid translocase (*Cd36*) (Figure 4C). In addition, plasma NEFA levels were increased by 2.3 fold in *Rarα*$^{Adi-/-}$ mice (Figure 4D). In contrast, there was no change in hepatic cholesterol, plasma TG or plasma cholesterol levels (Figure S1C–D). In addition, hepatic genes involved in fatty acid oxidation (*Pparα*, *Pparδ*, *Mcad*, *Cpt1*, *Cpt2*, *Pgc1α*), *Chrebp*, or phosphorylated AMPK levels were unchanged (Figure S1E–F).

We also measured hepatic de novo lipogenesis by giving mice heavy water followed by GC-MS analysis. Consistent with the changes in hepatic gene expression, loss of adipocyte RARα increased hepatic palmitate and triglyceride synthesis by 143% and 225%, respectively (Figure 4E).

Finally, we investigated the direct crosstalk between adipocytes and hepatocytes in a co-culture study involving primary adipocytes and primary hepatocytes. Our data showed that loss of RARα in adipocytes induced *Srebp1c*, *Acc1*, *Acc2*, *Cd36*, *Plin2*, *Plin4* and *Cidea* expression in hepatocytes (Figure 4F), indicating that adipocyte RARα has a profound impact on the expression of hepatocytic genes involved in lipogenesis, fatty acid uptake and lipid droplet formation. Taken together, our data suggest that loss of adipocyte RARα induces hepatic lipid accumulation likely by inducing hepatic lipogenesis.

Adipocyte RARα deficiency exacerbates HFD-induced non-alcoholic steatohepatitis

Rarα$^{Adi-/-}$ mice have FFA accumulation in the liver (Figure 4A), which may cause lipotoxicity and the progression of NAFLD. Consistent with this hypothesis, *Rarα*$^{Adi-/-}$ mice had elevated plasma levels of aspartate aminotransferase (AST) and alanine aminotransferase (ALT) (Figure 5A) and hepatic levels of reactive oxygen species (ROS) (Figure 5B). *Rarα*$^{Adi-/-}$ mice also had increased hepatic hydroxyproline levels (Figure 5C), liver fibrosis, DNA fragmentation (Figure 5D–E), and monocyte/Kupffer cell accumulation (Figure 5F–G). DNA fragmentation is a key feature of apoptosis, and apoptosis and inflammation play a key role in NAFLD progression (24, 25). In line with these findings, hepatic mRNA levels of collagen type 1, alpha 1 (*Col1a1*) and *Col1a2* (Figure 5H) as well as phosphorylated SMAD2 and SMAD2 and cleaved caspase 3 levels (Figure 5I–J) were significantly induced. Thus, loss of adipocyte RARα promotes NASH development likely by inducing ROS production and liver injury/apoptosis.

Loss of adipocyte RARα promotes obesity and NASH in aged chow-fed mice

The data of Figures 2–5 were collected from HFD-fed mice. We also investigated whether similar observations could be seen in aged mice. In 12-month-old, chow-fed mice, loss of adipocyte RARα led to increased obesity, reduced thermogenesis, unchanged activity, increased lipogenesis in WAT (Figure S2A–F), and increased NASH development (Figures S2A–F and S3A–F). Thus, our data indicate that adipocyte RARα is essential for protecting against obesity-associated NAFLD.

Adipocyte RARα inhibits lipogenesis and adiponectin signaling in adipocytes

Fatty acid influx from adipose tissue into hepatocytes plays a key role in the pathogenesis of NAFLD. In adipose tissue of HFD-fed $Rara^{Adi-/-}$ mice, lipogenic genes (*Srepb1c*, fatty acid synthase (*Fasn*), *Acc1*, *Acc2*, *Scd1*) were significantly induced, adipose triglyceride lipase (*Atgl*) was unchanged, and adiponectin (*Adipoq*) and hormone-sensitive lipase (*Hsl*) were repressed (Figure 6A). Adiponectin may function through activating AMP-activated protein kinase (AMPK) (26, 27). Indeed, in both WAT and BAT of $Rara^{Adi-/-}$ mice, phosphorylated AMPK (pAMPK) levels were significantly reduced (Figure 6B). Plasma adiponectin levels were also reduced (Figure 6C). Transient transfection studies showed that RARα induced adiponectin promoter activity (Figure 6D), suggesting that RARα regulates adiponectin gene transcription directly.

In primary adipocytes, loss of RARα significantly induced mRNA levels of lipogenic genes, including *Srebp1c*, *Fasn*, *Acc1*, and *Acc2* (Figure 6E). Western blot assays showed that loss of RARα in primary adipocytes reduced pAMPK levels and induced SREBP1C and ACC protein levels whereas phospho-HSL or ATGL protein levels were unchanged (Figure 6F–G). Consistent with the changes in gene expression, loss of RARα had no effect on lipolysis (Figure 6H), but increased de novo lipogenesis by >2 fold in primary adipocytes (Figure 6I). Thus, loss of adipocyte RARα enhances the release of FFAs from adipose tissue likely by inducing lipogenesis in adipose tissue (Figure 6) and inhibiting thermogenesis (Figure 2).

Adipocyte RARα deficiency exacerbates low-grade chronic inflammation

Hypertrophic adipocytes may release inflammatory cytokines that may in turn contribute to NASH development. Therefore, we investigated whether the loss of RARα in adipocytes caused chronic inflammation. $Rara^{Adi-/-}$ mice had increased expression of inflammatory genes in adipose tissue (Figure 7A) or the liver (Figure 7B), including tumor necrosis factor alpha (*Tnf*α), interleukin 1 beta (*Il-1β*), transforming growth factor beta (*Tgfβ*) and/or monocyte chemoattractant protein *(Mcp1*). Plasma levels of TNFα, IL-1β, and MCP1 were also significantly increased (Figure 7C). Immunostaining of WAT with an F4/80 antibody showed that $Rara^{Adi-/-}$ mice had more crown-like structures (Figure 7D), suggesting more macrophage infiltration. In addition, primary adipocytes lacking *Rara* also had increased *Tnf*α and *Tgfβ* expression (Figure 7E). Co-culture of primary adipocytes with primary hepatocytes led to increased expression of *Mcp1* and *Tgfβ* (Figure 7F). Thus, loss of adipocyte RARα may directly cause hepatic inflammation.

Discussion

In this report, we used a genetic mouse model to demonstrate that adipocyte RARα plays an essential role in preventing the development of obesity and NAFLD in both aged mice or HFD-fed mice. Mechanistically, adipocyte RARα inhibits de novo lipogenesis (DNL) and inflammation and induces thermogenesis, which in turn affects the development and progression of NAFLD. Since adipose RARα expression is reduced in obese mice, the reduced RARα expression in adipose tissue may contribute to the development of obesity-associated NAFLD.

Lipolysis in adipose tissue is known to play a key role in raising plasma FFA levels during fasting or insulin resistance. However, our data show that adipose RARα does not regulate insulin resistance or the expression of key lipolytic genes (ATGL, HSL) or lipolysis in vitro or ex vivo, suggesting that lipolysis may not play a major role in raising plasma FFA levels in $Rara^{Adi-/-}$ mice. Nonetheless, lipolysis may contribute to the elevated plasma FFA levels and NAFLD phenotype if adiposity and insulin resistance are aggravated in $Rara^{Adi-/-}$ mice. Our data suggest that loss of adipocyte RARα leads to increased lipogenesis and reduced thermogenesis, which may account for the increase in plasma FFA levels.

Our in vivo, in vitro, and co-culture studies suggest that adipocyte RARα prevents the development and progression of NAFLD likely via reducing FFA influx into hepatocytes and low-grade inflammation. Reduced adiponectin signaling due to weight gain has been shown to cause NASH (28). Although plasma adiponectin levels are reduced in $Rara^{Adi-/-}$ mice, hepatic pAMPK levels or genes involved in fatty acid oxidation (FAO) are unchanged, suggesting that adiponectin signaling may not regulate NASH development directly. Nonetheless, adipose adiponectin-AMPK signaling is impaired in $Rara^{Adi-/-}$ mice, which may contribute to the increased lipogenesis in adipose tissue. The influx of FFAs from adipose tissue, together with systemic low-grade inflammation and increased hepatic DNL likely due to delayed glucose clearance, may cause lipotoxicity, ROS production, and apoptosis in the liver of $Rara^{Adi-/-}$ mice, leading to the development and progression of NAFLD. We have previously shown that loss of RARα in hepatocytes induces hepatosteatosis via inhibiting lipid droplet formation and inducing fatty acid uptake (29). Thus, adipocyte RARα and hepatocyte RARα regulate the development of hepatosteatosis via distinct mechanisms.

Adipocyte RARα regulates plasma fatty acid levels likely via inhibiting de novo lipogenesis (DNL) and inducing thermogenesis. In adipocytes of $Rara^{Adi-/-}$ mice, the impaired adiponectin-AMPK pathway may account, at least in part, for the increased DNL. RARα regulates adiponectin and UCP1 promoter activities, suggesting a direct regulation of these two genes. It is likely that other mechanisms are also involved in RARα-regulated DNL and thermogenesis in adipose tissue.

In summary, we have demonstrated that adipocyte RARα plays a protective role in preventing obesity and NAFLD by inhibiting lipogenesis and inflammation and by inducing thermogenesis. Given that RAR signaling is relatively conserved between humans and mice, targeting adipocyte RARα may provide a novel approach to treat obesity and obesity-associated NAFLD. Nonetheless, only male mice were used in the current study, which is one of the study limitations.

Supplementary Material

Refer to Web version on PubMed Central for supplementary material.

Acknowledgements

We thank Dr. Yasmine Balkaid (NIH/NIAID) for sharing Rara$^{fl/fl}$ mice. We also thank Dr. Laurent Vergnes (University of California Los Angeles, Los Angeles, CA) for the pGL3-Ucp1-2.3kb plasmid and Dr. Jianhua Shao (University of California San Diego, La Jolla, CA) for the pGL3-Adiponectin-3kb plasmid.

Financial support and sponsorship:

This work was funded in part by NIH grants R01DK121548 and R01DK102619.

Data available

All data are available upon request.

Abbreviations:

9-cis-RA	9-cis retinoic acid
ACC	acetyl-CoA carboxylase
ADIPOQ	adiponectin
ALT	alanine aminotransferase
AMPK	AMP-activated protein kinase
AST	aspartate aminotransferase
ATGL	adipose triglyceride lipase
AtRA	all-trans retinoic acid
BAT	brown adipose tissue
CD36	cluster of differentiation 36
CIDE	cell death-inducing DFFA like effector
COL1A1	collagen type1 a1
DNL	de novo lipogenesis
eWAT	epididymal white adipose tissue
FASN	fatty acid synthase
FC	free cholesterol
GTT	glucose tolerance test
HFD	high fat diet
HSL	hormone sensitive lipase
IL-1β	interleukin 1β
ITT	insulin tolerance test

iWAT	inguinal white adipose tissue
MCP1	monocyte chemoattractant protein 1
NAFLD	non-alcoholic fatty liver disease
NASH	non-alcoholic steatohepatitis
NEFA	non-esterified free fatty acids
OCA	oxygen consumption rate
PGC1α	peroxisome proliferator-activated receptor coactivator 1α
PLIN	perilipin
PPARγ	peroxisome proliferator-activated receptor γ
RARE	retinoic acid response element
RARα	retinoic acid receptor α
RER	respiratory exchange ratio
ROS	reactive oxygen species
RXR	retinoic X receptor
SCD1	stearoyl-CoA desaturase
SREBP1	sterol regulatory element-binding protein 1
SVF	stromal vascular fraction
TC	total cholesterol
TGFβ	transforming growth factor β
TIMP1	tissue inhibitor of matrix metalloproteinase 1
TNFα	tumor necrosis factor α
UCP1	uncoupled protein 1

References

1. Wang Y, Beydoun MA, Min J, Xue H, Kaminsky LA, Cheskin LJ. Has the prevalence of overweight, obesity and central obesity levelled off in the United States? Trends, patterns, disparities, and future projections for the obesity epidemic. Int J Epidemiol 2020;49:810–823. [PubMed: 32016289]
2. Clinical guidelines on the identification, evaluation, and treatment of overweight and obesity in adults: executive summary. Expert Panel on the Identification, Evaluation, and Treatment of Overweight in Adults. Am J Clin Nutr 1998;68:899–917. [PubMed: 9771869]
3. Zhang Y, Li R, Li Y, Chen W, Zhao S, Chen G. Vitamin A status affects obesity development and hepatic expression of key genes for fuel metabolism in Zucker fatty rats. Biochem Cell Biol 2012;90:548–557. [PubMed: 22554462]

4. Zulet MA, Puchau B, Hermsdorff HH, Navarro C, Martinez JA. Vitamin A intake is inversely related with adiposity in healthy young adults. J Nutr Sci Vitaminol (Tokyo) 2008;54:347–352. [PubMed: 19001764]
5. Botella-Carretero JI, Balsa JA, Vazquez C, Peromingo R, Diaz-Enriquez M, Escobar-Morreale HF. Retinol and alpha-tocopherol in morbid obesity and nonalcoholic fatty liver disease. Obes Surg 2010;20:69–76. [PubMed: 18830789]
6. Suano de Souza FI, Silverio Amancio OM, Saccardo Sarni RO, Sacchi Pitta T, Fernandes AP, Affonso Fonseca FL, Hix S, et al. Non-alcoholic fatty liver disease in overweight children and its relationship with retinol serum levels. Int J Vitam Nutr Res 2008;78:27–32. [PubMed: 18654951]
7. Newsome PN, Beldon I, Moussa Y, Delahooke TE, Poulopoulos G, Hayes PC, Plevris JN. Low serum retinol levels are associated with hepatocellular carcinoma in patients with chronic liver disease. Aliment Pharmacol Ther 2000;14:1295–1301. [PubMed: 11012474]
8. Ghyselinck NB, Duester G. Retinoic acid signaling pathways. Development 2019;146.
9. Cassim Bawa FN, Zhang Y. Retinoic acid signaling in fatty liver disease. Liver Res 2023.
10. Rochette-Egly C, Germain P. Dynamic and combinatorial control of gene expression by nuclear retinoic acid receptors (RARs). Nucl Recept Signal 2009;7:e005. [PubMed: 19471584]
11. Lee SA, Jiang H, Feranil JB, Brun PJ, Blaner WS. Adipocyte-specific expression of a retinoic acid receptor alpha dominant negative form causes glucose intolerance and hepatic steatosis in mice. Biochem Biophys Res Commun 2019;514:1231–1237. [PubMed: 31109648]
12. Chapellier B, Mark M, Messaddeq N, Calleja C, Warot X, Brocard J, Gerard C, et al. Physiological and retinoid-induced proliferations of epidermis basal keratinocytes are differently controlled. EMBO J 2002;21:3402–3413. [PubMed: 12093741]
13. Zhang Y, Ge X, Heemstra LA, Chen WD, Xu J, Smith JL, Ma H, et al. Loss of FXR protects against diet-induced obesity and accelerates liver carcinogenesis in ob/ob mice. Mol Endocrinol 2012;26:272–280. [PubMed: 22261820]
14. Bligh EG, Dyer WJ. A rapid method of total lipid extraction and purification. Can J Biochem Physiol 1959;37:911–917. [PubMed: 13671378]
15. Roy D, Myers JM, Tedeschi A. Protocol for assessing exvivo lipolysis of murine adipose tissue. STAR Protoc 2022;3:101518. [PubMed: 35779261]
16. Galmozzi A, Kok BP, Saez E. Isolation and Differentiation of Primary White and Brown Preadipocytes from Newborn Mice. J Vis Exp 2021.
17. Cassim Bawa FN, Gopoju R, Xu Y, Hu S, Zhu Y, Chen S, Jadhav K, et al. Retinoic Acid Receptor Alpha (RARalpha) in Macrophages Protects from Diet-Induced Atherosclerosis in Mice. Cells 2022;11.
18. Oeckl J, Bast-Habersbrunner A, Fromme T, Klingenspor M, Li Y. Isolation, Culture, and Functional Analysis of Murine Thermogenic Adipocytes. STAR Protoc 2020;1:100118. [PubMed: 33377014]
19. O'Connor S, Cohen P. In Vitro Approaches to Model and Study Communication Between Adipose Tissue and the Liver. Methods Mol Biol 2017;1566:151–158. [PubMed: 28244049]
20. Vergnes L, Lin JY, Davies GR, Church CD, Reue K. Induction of UCP1 and thermogenesis by a small molecule via AKAP1/PKA modulation. J Biol Chem 2020;295:15054–15069. [PubMed: 32855239]
21. Mina AI, LeClair RA, LeClair KB, Cohen DE, Lantier L, Banks AS. CalR: A Web-Based Analysis Tool for Indirect Calorimetry Experiments. Cell Metab 2018;28:656–666 e651. [PubMed: 30017358]
22. Redonnet A, Bonilla S, Noel-Suberville C, Pallet V, Dabadie H, Gin H, Higueret P. Relationship between peroxisome proliferator-activated receptor gamma and retinoic acid receptor alpha gene expression in obese human adipose tissue. Int J Obes Relat Metab Disord 2002;26:920–927. [PubMed: 12080444]
23. Li Y, Fromme T, Schweizer S, Schottl T, Klingenspor M. Taking control over intracellular fatty acid levels is essential for the analysis of thermogenic function in cultured primary brown and brite/beige adipocytes. EMBO Rep 2014;15:1069–1076. [PubMed: 25135951]
24. Loomba R, Friedman SL, Shulman GI. Mechanisms and disease consequences of nonalcoholic fatty liver disease. Cell 2021;184:2537–2564. [PubMed: 33989548]

25. Pan X, Zhang Y. Hepatocyte nuclear factor 4alpha in the pathogenesis of non-alcoholic fatty liver disease. Chin Med J (Engl) 2022;135:1172–1181. [PubMed: 35191422]

26. Yamauchi T, Kamon J, Minokoshi Y, Ito Y, Waki H, Uchida S, Yamashita S, et al. Adiponectin stimulates glucose utilization and fatty-acid oxidation by activating AMP-activated protein kinase. Nat Med 2002;8:1288–1295. [PubMed: 12368907]

27. Tomas E, Tsao TS, Saha AK, Murrey HE, Zhang Cc C, Itani SI, Lodish HF, et al. Enhanced muscle fat oxidation and glucose transport by ACRP30 globular domain: acetyl-CoA carboxylase inhibition and AMP-activated protein kinase activation. Proc Natl Acad Sci U S A 2002;99:16309–16313. [PubMed: 12456889]

28. Handa P, Maliken BD, Nelson JE, Morgan-Stevenson V, Messner DJ, Dhillon BK, Klintworth HM, et al. Reduced adiponectin signaling due to weight gain results in nonalcoholic steatohepatitis through impaired mitochondrial biogenesis. Hepatology 2014;60:133–145. [PubMed: 24464605]

29. Cassim Bawa FN, Xu Y, Gopoju R, Plonski NM, Shiyab A, Hu S, Chen S, et al. Hepatic retinoic acid receptor alpha mediates all-trans retinoic acid's effect on diet-induced hepatosteatosis. Hepatol Commun 2022;6:2665–2675. [PubMed: 35852305]

Study Importance

What is already known?

- Retinoic acid signaling plays an important role in development and metabolism
- Hepatic RARα inhibits the development of NAFLD.
- Macrophage RARα inhibits the development of atherosclerosis.

What does this study add?

- Adipose RARα is reduced in *db/db* or *ob/ob* mice.
- Adipocyte RARα protects against obesity and steatohepatitis
- Adipocyte RARα inhibits lipogenesis and inflammation and induces thermogenesis

How might these results change the direction of research?

- Our studies suggest that activation of adipocyte RARα signaling may help to prevent obesity and steatohepatitis.

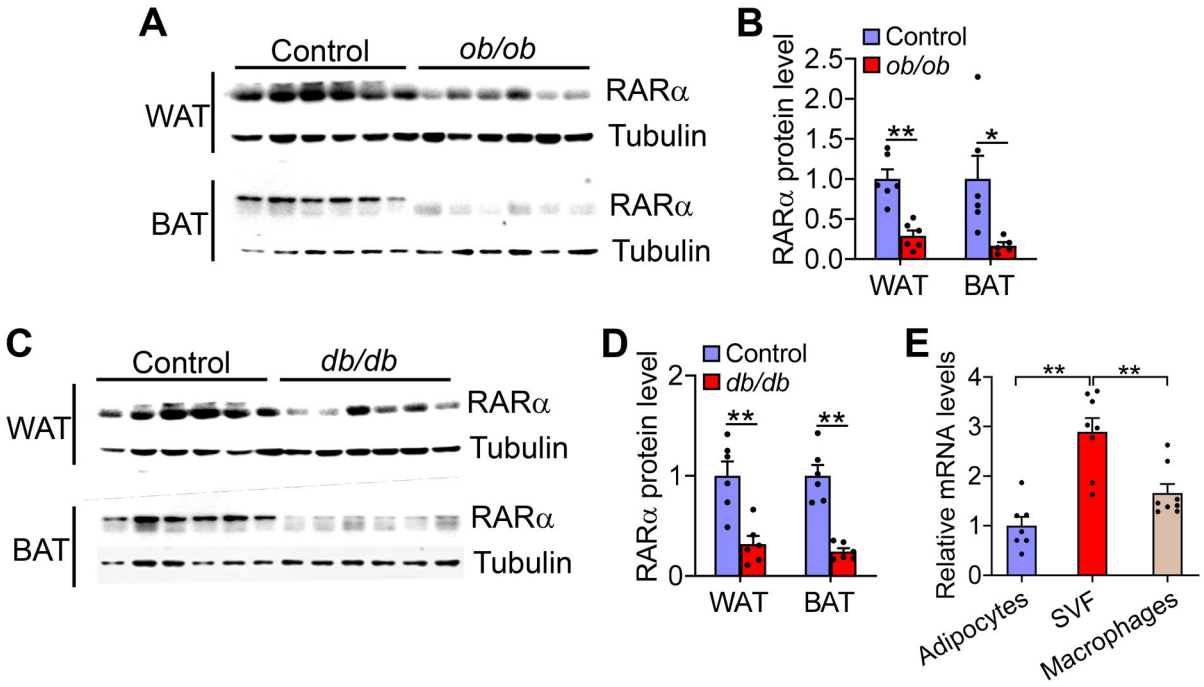

Figure 1. Adipose RARα levels are reduced in *ob/ob* or *db/db* mice

(**A-B**) RARα protein levels in white adipose tissue (WAT) and brown adipose tissue (BAT) of *ob/ob* mice were analyzed by Western blot assays (**A**) and then quantified (**B**) (n=6 per group) (**C-D**) RARα protein levels in WAT and BAT of *db/db* mice (n=6 per group). (**E**) mRNA levels of *Rarα* in white adipocytes, stromal Vascular fraction (SVF), and macrophages in two-month-old C57BL/6J male mice were quantified (n=8). Data are expressed as mean±SEM. Statistical analysis was performed using a 2-tailed, unpaired *t*-test. **P*<0.05, ***P*<0.01 versus controls

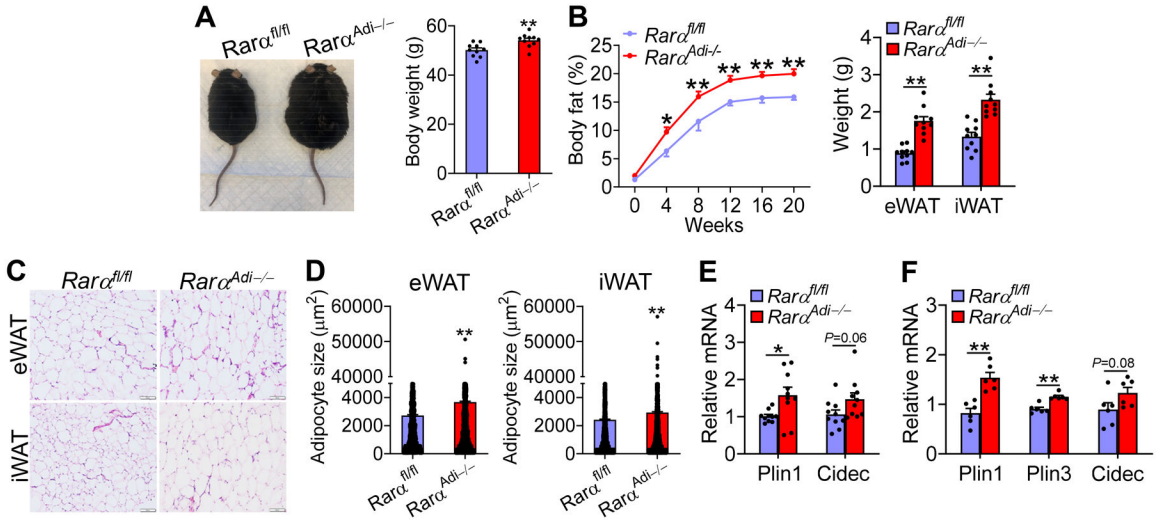

Figure 2. Adipocyte RARα deficiency exacerbates HFD-induced obesity

(**A-E**) *Rarα*$^{fl/fl}$ mice and *Rarα*$^{Adi-/-}$ mice were fed a high fat diet (HFD) for 20 weeks (n=10). (**A**) Representative images of mice (left panel) and body weight (right panel) at 20 weeks. (**B**) Body fat content at indicated time points (left panel) and epididymal white adipose tissue (eWAT) weight (left) or inguinal WAT (iWAT) weight (right) at 20 weeks. (**C**) Representative H&E staining of eWAT (top panel) and iWAT (bottom panel). (**D**) Adipocyte size of eWAT (left panel) and iWAT (right panel). (**E**) mRNA levels in WAT. (**F**) Primary adipocyte stem cells were isolated from *Rarα*$^{fl/fl}$ mice and *Rarα*$^{Adi-/-}$ mice. Following induction of adipogenesis, mRNA levels were quantified (n=6). Scale bars in **C**: 100 μm. Data are expressed as mean±SEM. Statistical analysis was performed using a 2-tailed, unpaired *t*-test in **A**, **B** (right panel), **D-F,** or two-way ANOVA with Šídák's multiple comparisons in **B** (left panel). **P*<0.05, ***P*<0.01 versus controls

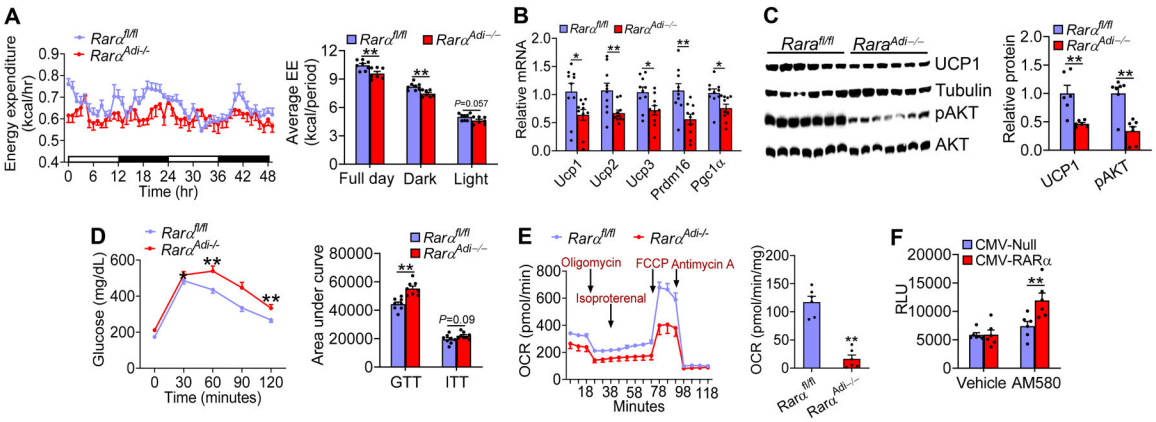

Figure 3. Adipocyte RARα deficiency decreases energy expenditure and UCP-dependent thermogenesis

(**A-D**) *Rara*$^{fl/fl}$ mice and *Rara*$^{Adi-/-}$ mice were fed a high fat diet (HFD) for 20 weeks (n=10). Hourly energy expenditure (EE) over 50 hours (left panel) and the average energy expenditure during the light and dark cycles (right panel) at 16 weeks were determined (**A**). mRNA levels (**B**) and protein levels (**C**) in BAT were determined. Glucose tolerance test (GTT) (left panel) was performed and area under curve of GTT and insulin tolerance test (ITT) was calculated (right panel) (**D**). In (**C**), pAKT and total AKT levels in BAT were measured 15 minutes after mice were injected with insulin (n=7). (**E**) Primary brown adipocytes were isolated from *Rara*$^{fl/fl}$ mice and *Rara*$^{Adi-/-}$ mice. Oxygen consumption rate (OCR) was determined after treatment with indicated chemicals (left panel), and UCP1-dependent OCR was quantified (right panel) (n=6). (**F**) A 2.3-kb *Ucp1* promoter-luciferase construct together with CMV-Null or CMV-RARα was transfected into 3T3-L1 cells, and then treated with either vehicle or AM580 (a RARα-selective agonist) for 24 h (n=6). Relative luciferase units (RLU) were determined. Data are expressed as mean±SEM. Statistical analysis was performed using a 2-tailed, unpaired *t*-test in **A** (right panel), **B, D-F**, or two-way ANOVA with Tukey's multiple comparison tests (**A**, left panel). **P*<0.05, ***P*<0.01, versus controls

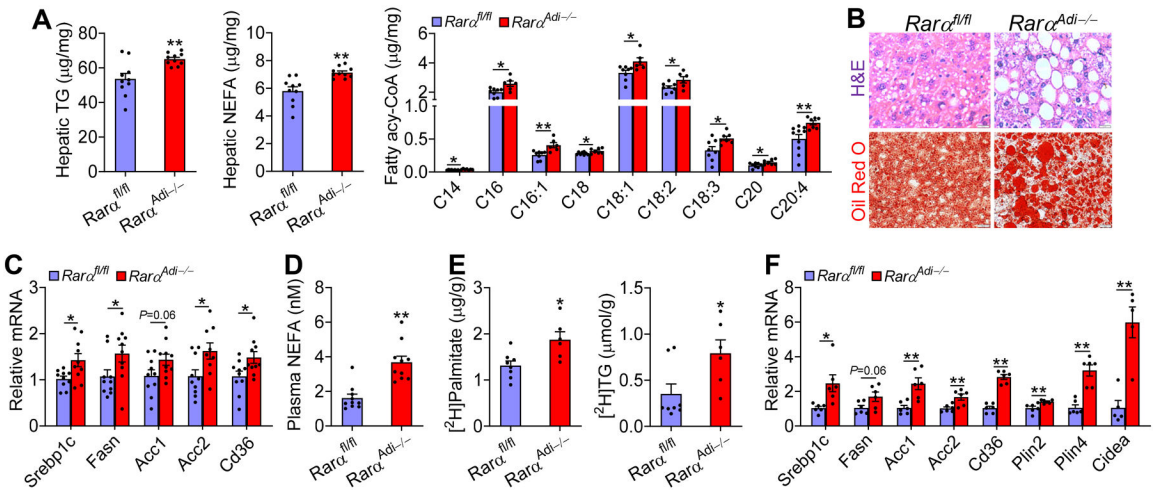

Figure 4. Adipocyte RARα deficiency exacerbates HFD-induced lipid accumulation through increasing lipogenesis

(**A-D**) *Rarα*$^{fl/fl}$ mice and *Rarα*$^{Adi-/-}$ mice were fed a high fat diet (HFD) for 20 weeks (n=10). Hepatic TG levels (left panel), NEFA levels (middle panel), and fatty acid composition (right panel) were determined (**A**). Liver sections were stained with hematoxylin and eosin (H&E) staining (top panel) or Oil red O (ORO) (lower panel) (**B**). Hepatic mRNA (**C**) and plasma NEFA (**D**) levels were analyzed. (**E**) *Rarα*$^{fl/fl}$ mice and *Rarα*$^{Adi-/-}$ mice were fed an HFD for 12 weeks and also given heavy water (n=6–8). Newly synthesized hepatic palmitate (left panel) and TG (right panel) levels were determined. (**F**) Primary hepatocytes isolated from C57BL/6J mice were co-cultured with primary adipocytes isolated from *Rarα*$^{fl/fl}$ mice and *Rarα*$^{Adi-/-}$ mice for 48 hours (n=6), and mRNA levels were determined. Scar bars in **B** equal to 20 μm. Data are expressed as mean±SEM. Statistical analysis was performed using a 2-tailed, unpaired *t*-test. **P*<0.05, ***P*<0.01 versus controls

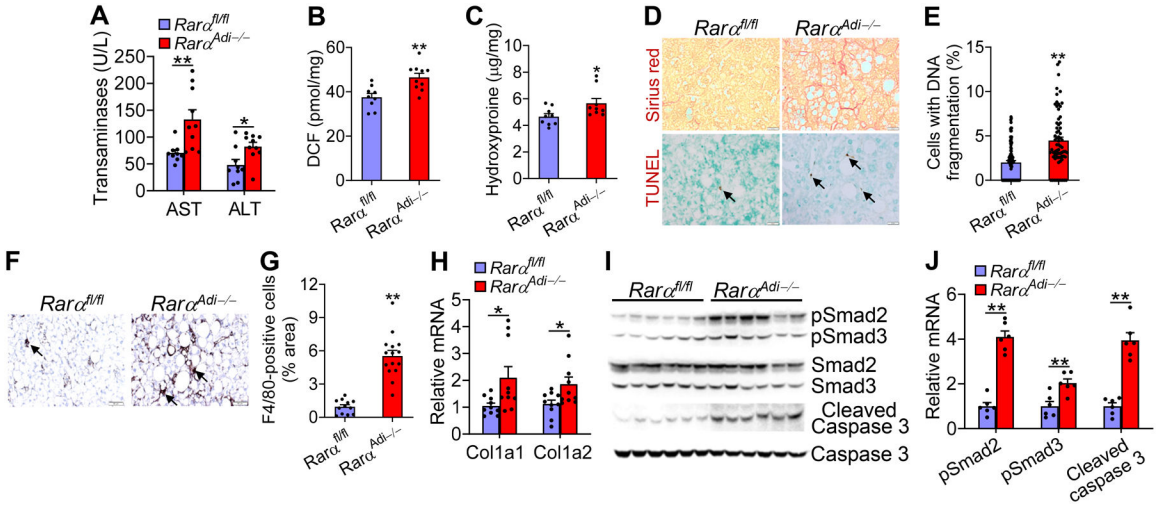

Figure 5. Adipocyte RARα deficiency exacerbates HFD diet-induced non-alcoholic steatohepatitis

Rarα$^{fl/fl}$ mice and *Rarα*$^{Adi-/-}$ mice were fed a high fat diet (HFD) for 20 weeks (n=10). (**A**) Plasma transaminase levels. (**B**) Hepatic ROS levels. (**C**) Hepatic hydroxyproline levels. (**D**) Liver sections stained with Picrosirius red (top panel) or subjected to TUNEL assays (bottom panel). (**E**) Hepatic cells with DNA fragmentation (%). (**F-G**) Liver sections were stained with an F4/80 antibody (**F**) and F4/80-positive areas (%) were quantified (**G**). (**H**) Hepatic mRNA levels. (**I-J**) Hepatic protein levels were analyzed by Western blot assays (**I**) and then quantified (**J**). In (**D**), arrows point to cells with DNA fragmentation, and scale bars equal to 20 μm. In (**F**), arrows point to F4/80-positive cells, and scale bars equal to 50 μm. Data are expressed as mean±SEM. Statistical analysis was performed using a 2-tailed, unpaired *t*-test. **P*<0.05, ***P*<0.01 versus controls

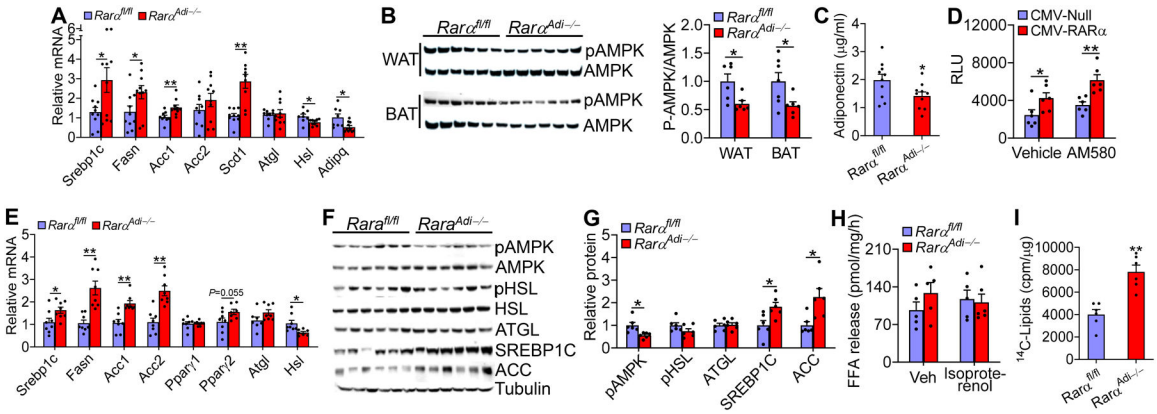

Figure 6. Adipocyte RARα regulates lipogenesis and adiponectin signaling in adipocytes

(**A-C**) *Rarα*$^{fl/fl}$ mice and *Rarα*$^{Adi-/-}$ mice were fed a high fat diet (HFD) for 20 weeks (n=10). mRNA levels in WAT (**A**) and protein levels in WAT and BAT (**B,** left and right panels) were determined. Plasma adiponectin levels (**C**) and adiponectin promoter activity (**D**; n=6) were analyzed. (**E-G**) Primary adipocyte stem cells were isolated from *Rarα*$^{fl/fl}$ mice and *Rarα*$^{Adi-/-}$ mice. After adipogenesis was induced, mRNA (**E**) and protein (**F-G**) levels were determined (n=6–8). (**H**) Lipolysis in adipose tissue of *Rarα*$^{fl/fl}$ mice and *Rarα*$^{Adi-/-}$ mice was determined in the presence or vehicle or 10 μM isoproterenol for 2 h (n=6–8). (**I**) *De novo* lipogenesis was performed in primary adipocyte stem cells in the presence of ^{14}C-acetic acid (n=6). Data are expressed as mean±SEM. Statistical analysis was performed using a 2-tailed, unpaired *t*-test. **P*<0.05, ***P*<0.01 versus controls

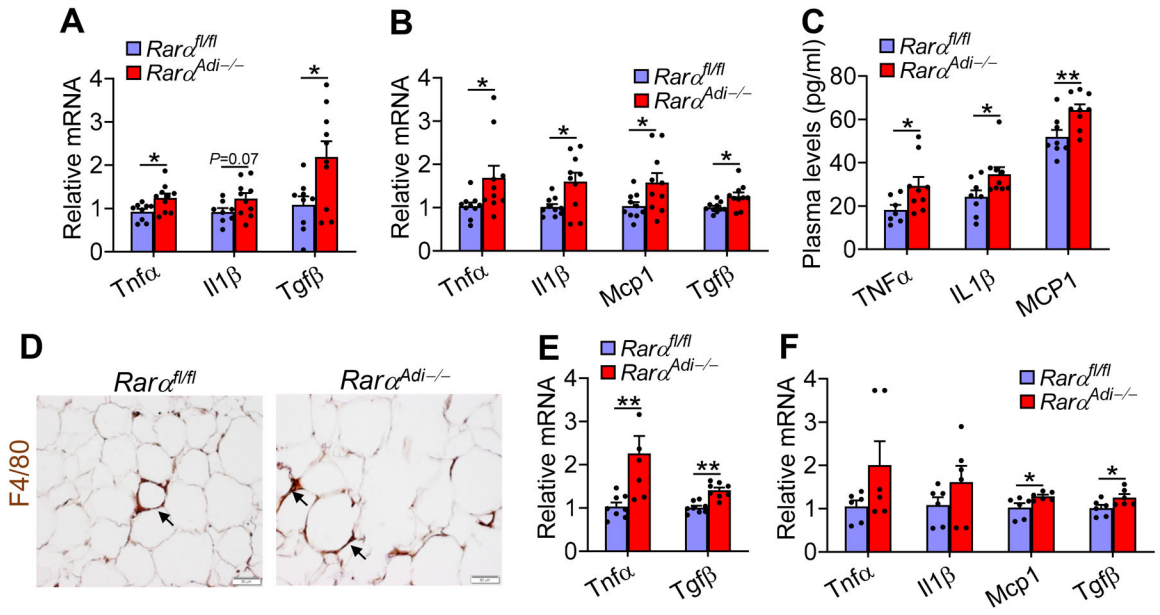

Figure 7. Adipocyte RARα deficiency exacerbates HFD-induced low-grade chronic inflammation

(**A-D**) *Rara*$^{fl/fl}$ mice and *Rara*$^{Adi-/-}$ mice were fed a high fat diet (HFD) for 20 weeks (n=10). mRNA levels in WAT (**A**) or the liver (**B**) as well as plasma inflammatory cytokine levels (**C**) were determined. The crown-like structure (CLS) in the WAT was shown after staining with an F4/80 antibody (**D**). (**E**) Primary adipocyte stem cells were isolated from *Rara*$^{fl/fl}$ mice and *Rara*$^{Adi-/-}$ mice, and mRNA levels were determined after adipogenesis was induced (n=7–8). (**F**) Primary hepatocytes isolated from C57BL/6 mice were co-cultured for 48 h with primary adipocytes isolated *Rara*$^{fl/fl}$ mice and *Rara*$^{Adi-/-}$ mice, and mRNA levels were determined (n=6). Scale bars in **D** equal to 50 μm. Data are expressed as mean±SEM. Statistical analysis was performed using a 2-tailed, unpaired *t*-test. **P*<0.05, ***P*<0.01 versus controls